crystals

MDPI

Review

Advancements in the Engineering Modification of Sucrose Phosphorylase

Shuru Ma [1,†], Hongyu Zhang [1,*,†], Tingting Lou [2] and Suying Wang [1,*]

[1] Tianjin Key Laboratory of Food Biotechnology, College of Biotechnology and Food Science, Tianjin University of Commerce, Tianjin 300134, China; 13038082139@163.com
[2] Key Laboratory of Industrial Fermentation Microbiology, Ministry of Education, Tianjin Key Laboratory of Industrial Microbiology, College of Biotechnology, Tianjin University of Science & Technology, Tianjin 300457, China; loutingtinggucas@126.com
* Correspondence: zhanghongyu@tjcu.edu.cn (H.Z.); wsying@tjcu.edu.cn (S.W.)
† These authors contributed equally to this work.

Abstract: Sucrose phosphorylase (SPase) is a member of the glycoside hydrolase family 13, catalyzing the reversible phosphorolysis of sucrose to produce α–glucose–1–phosphate and exhibiting transglycosylation activity toward multiple substrates. Its wide substrate specificity enables the synthesis of various glycosides, which are broadly applied in food, cosmetics, and pharmaceuticals. However, the industrial application of SPase is constrained by its poor thermostability and limited transglycosylation activity. Therefore, current research focuses on enhancing the thermostability and transglycosylation activity of SPase through efficient engineering strategies based on its crystal structure and catalytic mechanism. This paper systematically reviews the crystal structure and catalytic mechanism of SPase, outlines the application of protein engineering and immobilization strategies in improving the thermostability of SPase, and analyzes how modifications at key amino acid sites affect the synthesis of typical glycosylation products. It also summarizes the limitations of SPase engineering modification strategies and explores the potential of diversified approaches for SPase modification, highlighting its broad application prospects in industrial production and laying a solid foundation for further advancements in SPase engineering modification and its industrial application.

Keywords: sucrose phosphorylase; crystal structure; catalytic mechanism; thermostability; transglycosylation activity; engineering modification

check for updates

Citation: Ma, S.; Zhang, H.; Lou, T.; Wang, S. Advancements in the Engineering Modification of Sucrose Phosphorylase. *Crystals* **2024**, *14*, 972. https://doi.org/10.3390/cryst14110972

Academic Editors: Jasminka Kontrec, Anamarija Stanković, Martina Medvidović-Kosanović and Branka Njegić Džakula

Received: 1 October 2024
Revised: 29 October 2024
Accepted: 4 November 2024
Published: 9 November 2024

Copyright: © 2024 by the authors. Licensee MDPI, Basel, Switzerland. This article is an open access article distributed under the terms and conditions of the Creative Commons Attribution (CC BY) license (https://creativecommons.org/licenses/by/4.0/).

1. Introduction

Glycosides are widely distributed in nature and exhibit multiple biological activities. The enzymes responsible for the formation and breakdown of glycosidic bonds are classified into four types in the Carbohydrate–Active Enzymes (CAZy) database, including glycoside hydrolases (GHs), glycoside phosphorylases (GPs), transglycosidases (TGs), and glycosyltransferases (GTs) [1]. The GH13 family, commonly referred to as the α–amylase family, is the largest glycoside hydrolase family in the CAZy database [2]. SPase belongs to the GH13 family and catalyzes the phosphorolysis of sucrose and the reverse reaction, which is represented by the equation: Sucrose + phosphate ⇌ D–fructose + α–D–glucose–1–phosphate [3]. SPase is capable of transferring glucose moieties to specific acceptors such as water, phosphate, fructose, phenolic hydroxyl groups, and alcohol hydroxyl groups. It operates via a double–displacement mechanism, exhibiting broad acceptor specificity. SPase can transfer a glucose moiety from sucrose to various carbohydrate and non–carbohydrate substrates, synthesizing numerous high–value glycosides and oligosaccharides, such as 2–O–α–D–glucopyranosyl–α–D–glucose (kojibiose) [4], 3–O–α–D–glucopyranosyl–D–glucose (nigerose) [5], 2–O–(α–D–glucopyranosyl)–sn–glycerol (aGG) [6,7], and 2–O–α–D–glucopyranosyl–L–ascorbic acid (AA–2G) [8,9].

Therefore, SPase has broad application prospects in food, pharmaceuticals, and cosmetics [5,10–12]. The main synthetic products of SPase and their applications include the following aspects (Figure 1). (1) The synthesis of oligosaccharides: SPase can use glucose, xylose, rhamnose, galactose, fructose, etc., as acceptors to catalyze the synthesis of oligosaccharides with one additional glucose unit [13], which can be used in food additives, health products, dairy products for the elderly and infants, feed additives as well as probiotics [14,15]. (2) The synthesis of aGG: After the glycosylation of glycerol, αGG is obtained, which has moisturizing effects and can be used as a humectant in cosmetics and has potential as a health food ingredient and therapeutic agent [8]. (3) Improving the stability of certain substances: The glycosylation of ascorbic acid [16] and caffeic acid [17] by adding a glucose group significantly enhances the stability of ascorbic acid and caffeic acid, allowing them to perform more effectively. (4) The glycosylation of plant polyphenolic substances: SPase can glycosylate polyphenolic compounds like resveratrol [18], arbutin [19], phloretin [20], and catechin [21], enhancing their solubility, stability, and biological activity. (5) The glycosylation of other substances: SPase can transfer glucose groups to non–natural acceptors, including carotenoids and flavonoids [22]. However, the poor thermostability and limited transglycosylation activity of wild–type SPase from natural sources do not meet industrial application requirements. Therefore, mutation strategies such as directed evolution, semi–rational design, and rational design are needed to modify natural SPase to improve its stability and catalytic properties [23], enhancing its commercial application potential.

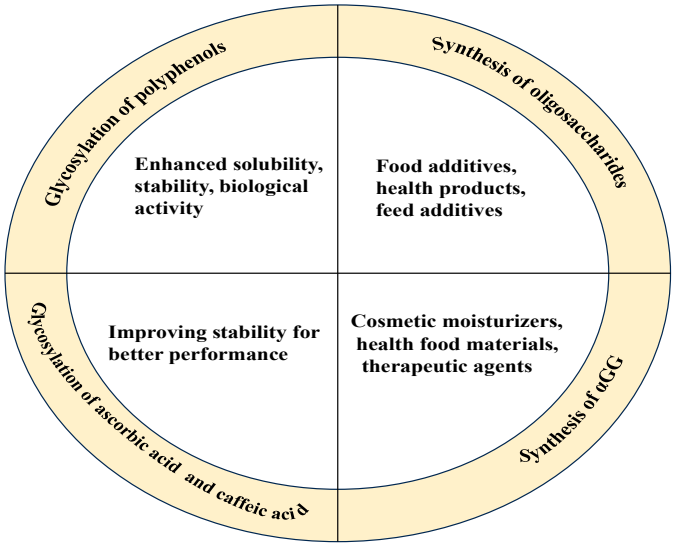


Figure 1. Application of products synthesized by SPase.

Based on this, this paper reviews the structure and catalytic mechanism of SPase, systematically summarizes recent advances in the engineering modification of SPase, and forecasts its application prospects, aiming to provide a reference for SPase basic research, applied research, and industrialization.

2. Structure and Catalytic Mechanism of SPase

SPase is composed of approximately 500 amino acids with a molecular weight ranging 50–60 kD [24]. SPases from different sources exhibit unique protein structures and substrate specificities. SPases from *Leuconostoc mesenteroides* and *Streptococcus mutans* (*Lm*SP and *Sm*SP) are monomeric proteins [25], while SPases from *Bifidobacterium adolescentis* DSM20083 (*Ba*SP) and *Pseudomonas saccharophila* are dimeric. In 2004, the crystal structure of *Ba*SP (PDB 2gdv) was resolved for the first time [26], marking the first crystal structure of SPase to be elucidated. ′ *Ba*SP contains four structural domains: As shown in Figure 2, BaSP contains four structural domains: A, B, B′and C [26], as shown in Table 1.

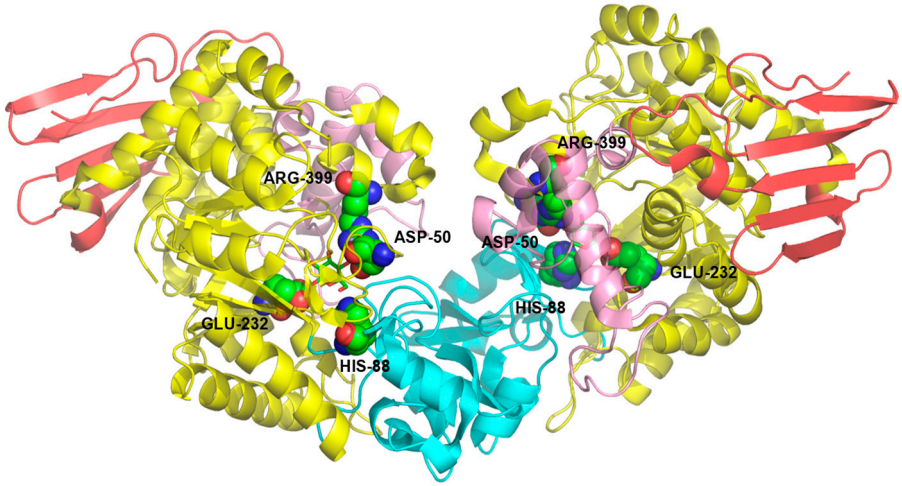


Figure 2. Crystal structure of *Ba*SP. Note: The images were generated by PyMOL2.6 software; different colors of folding represent different structural domains, yellow: structural domain A, blue–green: structural domain B, pink: structural domain B′, and red: structural domain C; The spheres represent the binding sites of *Ba*SP: Asp–50, HISHis–88, GLUGlu–232, ARGArg–399 (the protein is a dimer, the left and right structures are the same, and the residues are also the same); the stick structure represents the sucrose molecule.

Table 1. Domain composition of *Ba*SP.

Domain	Amino Acid	Structure
A	1–85, 167–291 and 356–435	Consisting of 8 alternating parallel β–strands (e1–e8) and α–helices (h1–h8) (β/α) 8–barrels
B	86–166	Two short antiparallel β–folding
B′	292–355	One long and one short α–helix
C	The first 56 amino acid residues at the C–terminus	A single–chain, five–stranded antiparallel beta–sheet

Domain A is a catalytic (β/α) 8–barrel structure commonly found in the GH13 family with the active sites Asp192 and Glu232 located at the tip of the (β/α) 8–barrel. Domains B and B′consist of two long loops formed by several amino acid residues within the (β/α) 8 barrel, acting as structural elements. Two flexible loops, Loop A (336AAASNLDLY344) and Loop B (132YRPRP136), located in Domains B and B′, are close to the catalytic center and are mainly involved in enzyme conformational changes during catalysis [27]. Most interactions are confined to the two B domains. The interaction between the loops in the two barrels leads to the formation of a large cavity in the dimer, which includes the substrate entry, with two active sites. The substrate channel along the active site pathway appears to be quite small, and one loop in Domain B′significantly contributes to the reduction in size, making the topology of Domain B′unfavorable for oligosaccharide binding, thus reducing the size of the substrate channel. Short hairpin loops connect chains 1–3 of Domain C, while the loop between chains 3 and 4 consists of 16 residues. The top of the loop is near Domain B′,partially hindering the oligosaccharide binding site in the SPase structure, making Domain C closely related to substrate specificity.

SPase is a versatile and efficient transglycosylation enzyme for two key reasons. First, its well–known acceptor promiscuity allows the glucosyl–enzyme intermediate to be captured by a variety of non–phosphate compounds, effectively transferring the glucose moiety of sucrose onto these compounds. Second, sucrose is a powerful donor with reactivity comparable to activated donors like UDP–glucose [28]. Therefore, the enzyme can achieve high transglycosylation yields. In recent years, researchers have detailed the reaction mechanism of SPase using methods such as enzyme crystal structure analysis and site–directed mutagenesis [1]. The catalytic mechanism of SPase is shown in Figure 3 [29].

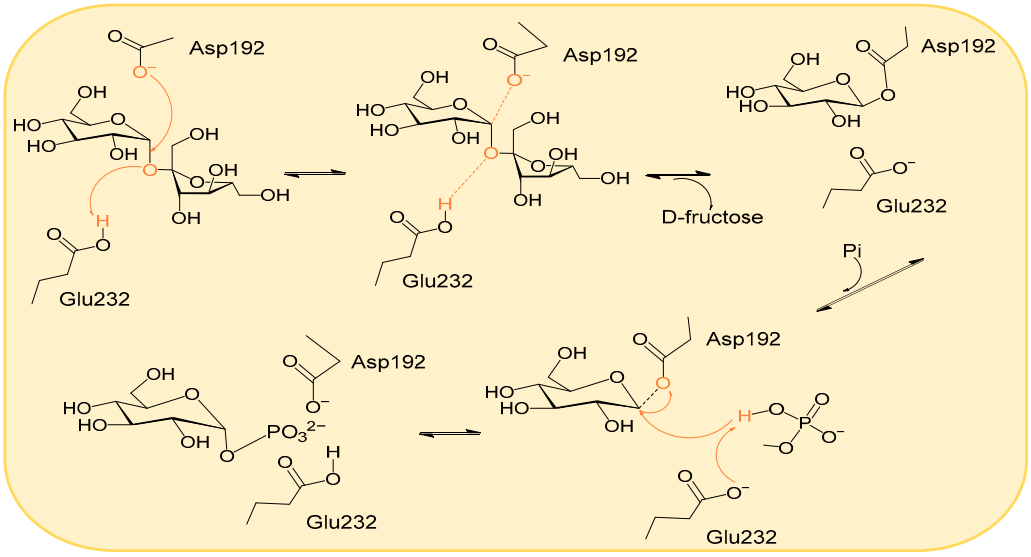


Figure 3. Catalytic reaction mechanism of SPase.

SPase performs transglycosylation reactions via a covalent intermediate and, like other enzymes in the family, follows a double–displacement mechanism during the reaction, as shown in Figure 4. In the double–displacement mechanism, two carboxylate amino acids (Asp192 [30] and Glu232 [31] in *Ba*SP) play key roles. These catalytic residues are fully conserved [32]. Asp192 (the catalytic nucleophile) attacks the anomeric carbon, while Glu232 (a general acid/base catalyst) protonates the oxygen of the glycosidic bond, leading to the formation of a covalent glycosyl–enzyme intermediate and the release of fructose. Once the acceptor site undergoes a conformational change, the intermediate can react with various acceptor substrates (water, inorganic phosphate, sugarsetc.), resulting in the release of glycoside products [26]. Mirza et al. studied the interaction of SPase with sucrose, as shown in Figure 5 [27].

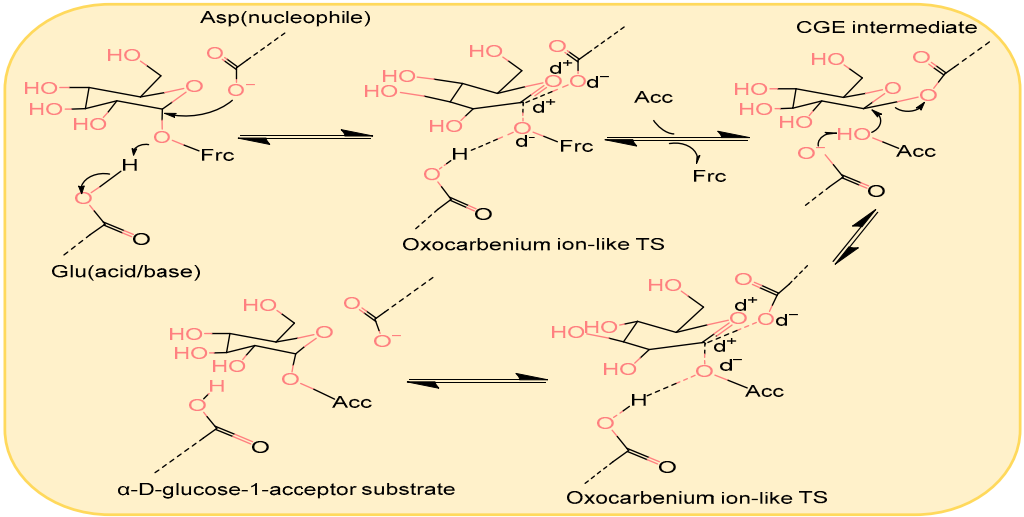


Figure 4. SPase general double–displacement reaction mechanism. Note: Frc represents the fructo–furanosyl part of sucrose; Acc represents the acceptor substrate; CGE represents the covalent glucosyl–enzyme intermediate.

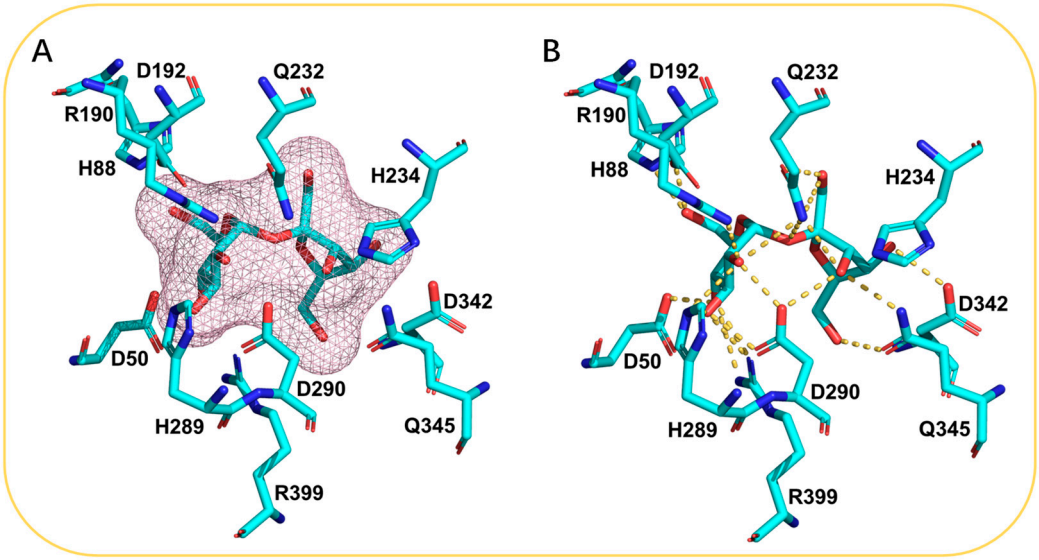


Figure 5. The interaction of SPase with sucrose. (**A**) Sucrose molecules bound in the active site pocket; (**B**) interaction of *Bi*SP (E232Q) and sucrose.

However, a major drawback of the double–displacement mechanism of SPase is that water in the reaction system reacts with the covalent intermediate of the glycosyl enzyme, leading to irreversible hydrolysis of the glycosyl donor substrate. As a result, during the catalysis of SPase, glycosylation competes with hydrolysis. The glucose generated by hydrolysis inhibits the catalytic activity of SPase, affecting the final yield. It is worth noting that hydrolysis, as a side reaction, is inevitable. To achieve optimal results, it is usually necessary to optimize the reaction conditions or perform enzyme engineering modifications to reduce hydrolysis and increase the proportion of glycosylation [26]. Unlike the hydrolysis reaction, the phosphate reaction is reversible, and Vyas and Nidetzky investigated the thermodynamic changes accompanying substrate binding in the base and transition states of glycosyl transfer in and out of the enzyme. The enzymatic glycosylation of sucrose and α–glucose 1–phosphate (Glc1P) was found to be rate–limiting in the forward (kcat = 84 s^{-1}) and reverse (kcat = 22 s^{-1}) directions of the reaction at 30 °C. Enzyme substrate binding was entropy–driven ($t\delta Sb \geq +23$ kJ/mol), possibly originating from enzyme desolvation at the binding site of the leaving group. The pathway from the ES complex to the transition state involves the absorption of heat ($\delta h^{\ddagger} = 72 \pm 5.2$ kJ/mol) with little further change in entropy. But the heat absorbed is about twice as much as that used during the formation of the enzyme–substrate complex. Thus, kcat/km, which represents the total enzyme conversion of the free substrate to the transition state, is strongly temperature dependent (more so than kcat), and it involves a significant increase in activation entropy, which almost matches the increase in entropy during substrate binding [33]. In the catalytic process of SPase, in addition to the catalytic residues, the residues of the catalytic subsites also play a key role. Wildberger et al. found that LmSP positions the enzyme–substrate Glc–1–P through hydrogen bonding with the catalytic triad and catalytic subsite Arg137 and that the amino acid residue Phe53 is critical for transition state stability [34]. Additionally, catalytic subsites Asp49 and Arg395 form a charged hydrogen bond network with the transferred glucosyl group, which promotes the catalytic reaction [35]. For example, the PDB databases of 7QQJ, 5MB2 and 6FME all show that hydrogen bonds can be formed between sucrose phosphorylase and the substrate. Certain sites significantly affect the catalytic efficiency of SPase, and thus effective mutation sites can be identified through computer–aided design and experimental validation, increasing enzyme activity.

3. Engineering Modifications of SPase

3.1. Thermostability Enhancement of SPase

For industrial applications, the conversion of carbohydrates is ideally conducted at 60 °C or above to prevent microbial contamination and excessive viscosity. However, SPase has only been found in a few non–thermophilic microorganisms. The SPase with the highest known thermostability is *Ba*SP–with an optimal reaction temperature of 58 °C [36]. This enzyme rapidly loses activity under industrial conditions at 60 °C [37]. Therefore, enhancing the thermostability of SPase is a key target for modification. With advancements in bioinformatics and high–throughput sequencing technologies, an increasing number of new enzymes have been discovered from thermophilic and hyperthermophilic bacteria, which are capable of withstanding the harsh conditions of industrial processes [38]. Comparing the sequences and crystal structures of enzymes from mesophilic and thermophilic bacteria shows high structural similarity (40~85%), with the key difference being that thermophilic proteins contain more charged hydrophobic residues and proline [39]. Over the past few decades, highly thermostable industrial enzymes have primarily been obtained through protein engineering, post–translational modifications, chemical modifications, additives, and immobilization [40,41]. With the deepening understanding of structure–function relationships and the development of computational tools, rational design [39,42] and semi–rational design have become effective methods for improving enzyme thermostability.

Additionally, immobilizing thermophilic enzymes on novel material carriers can significantly enhance their thermostability. At present, various strategies have been developed to improve the thermostability of SPase, including enzyme immobilization [43], as well as protein engineering strategies such as directed evolution, rational design [37], and semi–rational design [44,45] (Table 2).

Table 2. The engineering modification strategies for improving the thermostability of SPase.

Sources	Engineering Modification	Results	Ref.
Bifidobacterium adolescentis	Multipoint covalent immobilization	The optimal temperature of the enzyme is increased from 58 to 65 °C	[36]
Bifidobacterium adolescentis	Combination of sequence–and structure–based mutagenesis	The half–life at 60 °C increased dramatically from 24 to 62 h	[37]
Bifidobacterium adolescentis	CLEAs	The optimal temperature is increased by 17 °C	[43]
Streptococcus mutans	Random mutations	60% activity remains at 60 °C for 20 min	[46]
Bifidobacterium adolescentis	Alignment guided focused directed evolution	The library size could be significantly reduced while ensuring a high hit rate	[47]
–	–	–	
Leuconostoc mesenteroides	A semi–rational design strategy	The half– life has increased nearly two–fold	[48]
Leuconostoc mesenteroides	PROSS	Achieved high–level production of αGG	[49]
Bifidobacterium adolescentis	Sepabeads EC–HFA	The immobilized enzyme was able to retain 65% of its activity after 16 h incubation at 60 °C	[50]
Leuconostoc mesenteroides	Microstructured reactors	After 690 reactor cycles, the enzyme retains about 70% activity	[51]
Bifidobacterium adolescentis	iCLEA	Exhibiting altered acceptor specificity as well as excellent stability at 60 °C	[52]

3.1.1. Improving SPase Thermostability Through Protein Engineering

Combining sequence and structure was performed on *BaSP*. It is known that the aspartic acid residue cluster at positions 445–447 is the most flexible region, and sequence alignment revealed that D445 and D446 are structurally conserved target sites. Residues at positions 445 and 446 were simultaneously mutated to more common residues at these positions (Pro and Gly, or Pro and Thr). Studies indicated that the enzyme stability only increases.

For example, Fujii et al. employed an error–prone PCR random mutagenesis strategy and identified eight amino acid residues related to the thermostability of SPase from Streptococcus mutans. The mutant T47S/S62P/V128L/K140M/Y77H/Q144R/N155S/D249G, after combination mutations, showed a 20–fold increase in thermostability, indicating a synergistic effect of each mutation on the thermostability of enzyme. Sequence alignment suggests that these eight amino acid residues are located in the A domain of the enzyme and are distant from the active site [46]. The fully random mutagenesis strategy generates a large mutant library, which complicates screening. A directed evolution strategy was developed to reduce the library size. A B–Factor Iterative Test (B–FIT) was used to identify the most active site, which was then subjected to saturation mutagenesis. This site was used as a template to randomize another site, and the process was iterated until the desired improvement was achieved. However, this method remains limited by the size of the mutant library. Jochens et al., based on the B–FIT principle, proposed restricting site randomization to the most common amino acids in multiple sequence alignments. These amino acids are retained through natural selection and are generally believed to be more favorable for enzyme stability. This "smart library" method has been successfully applied to the modification of *Pseudomonas fluorescens* esterase, constructing a site–saturation library targeting three surface sites, reducing the number of screening colonies by 300–fold. Without affecting specific activity, several mutants with significantly improved stability were identified [47]. To identify mutants with higher kinetic stability, mutagenesis occurred when residues at positions 445 and 446 were mutated together, suggesting a synergistic effect between them [37].

Directed evolution does not require a deep understanding of the enzyme's structure and function but relies on efficient screening methods and extensive experimental work. Rational design requires a thorough understanding of protein structure and catalytic mechanisms. Semi–rational design combines the advantages of directed evolution and rational design, enabling high–quality mutants to be selected from a small library. Therefore, semi–rational design has become the preferred strategy for improving enzyme thermostability. Many studies have shown that changing a few amino acids can significantly enhance protein thermostability, especially with significant progress made using dPROSS–based methods [53–55]. By reducing the mutant library size, high–quality mutants can be screened more quickly, and as computational technologies merge with biological sciences, the efficiency of identifying beneficial mutation points is further enhanced. In recent years, an increasing number of semi–rational design strategies have been applied to improve enzyme thermostability. The *Lm*SPase has improved thermostability through FireProt 2.0 (a web server for multipoint thermostable mutation design as shown in Figure 6) [56,57] and semi–rational strategies such as structural–functional analysis and molecular dynamics simulations. Ultimately, a T219L single–point mutant with excellent thermostability was obtained [48].

The PROSS platform [58] offers a single–step design approach utilizing sequence information and Rosetta atomic modeling, with the result page functions illustrated in Figure 7. The simulated *Lm*SP crystal structure and homologous sequences were uploaded to the PROSS tool, which produced a mutation list. After selecting and validating appropriate mutation sites, the SPase mutants V23L and V23L/S424R with increased activity and stability were obtained. MD analysis revealed that the hydrophobic core formed by Leu23 stabilizes two α–helices of SPase (384–392 and 393–399) with the second α–helix embedded and near the active sites (D196 and E237). Since the hydrophobic core formed by Leu23 is relatively stable, and this region is close to the active center, it may significantly affect the thermostability of SPase [49].

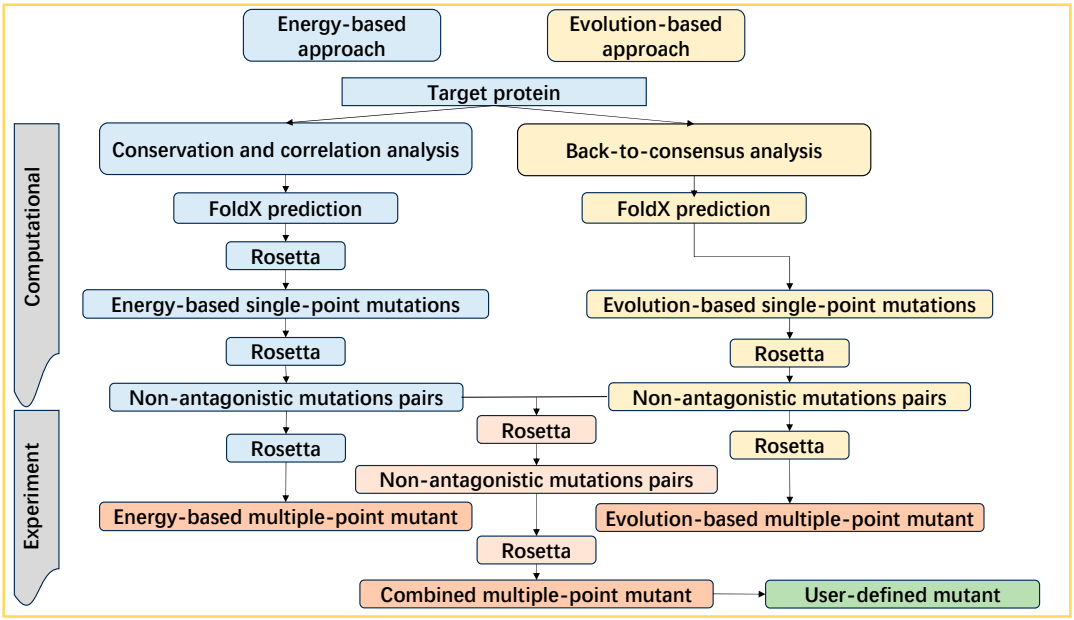


Figure 6. Workflow of FireProt strategy MD analysis indicated that all residues in contact with L219 are close to the active sites (D196 and E237), and L219 is situated in the hydrophobic protein core, which is resistant to high temperatures. Additionally, the PROSS method can be used to construct mutants with higher thermostability.

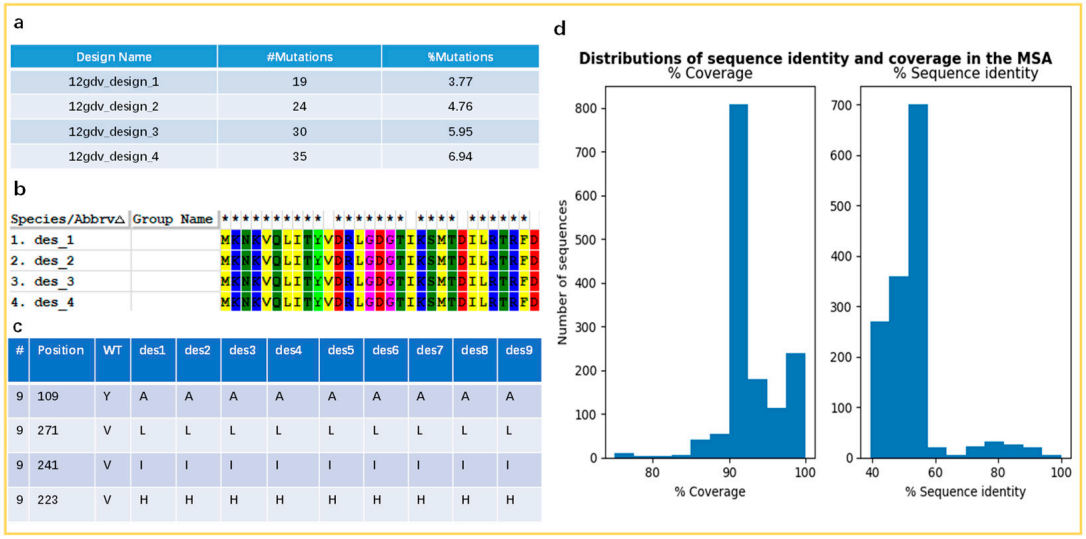


Figure 7. Features from the PROSS2 results page. (**a**) A tabular summary of designs. (**b**) Sequence view comparing all designs to the query (An asterisk indicates that this column of residue letters is completely conservative). (**c**) Part of a table reporting the identities at all mutated positions across the designs. (**d**) Histograms depicting the quality of the multiple sequence alignment according to their sequence diversity and coverage relative to the query sequence. Note: The asterisk indicates that this column of residue is completely conservative.

3.1.2. Thermostability Modification of SPase Based on Immobilization Strategy

In addition to protein engineering modifications, immobilization is also an effective strategy for enhancing enzyme thermostability [59]. The SPase (*Ba*SP) from *Bifidobacterium adolescentis* was immobilized via multipoint covalent attachment on Sepabeads EC–HFA (Figure 8), and its optimal reaction temperature increased from 58 to 65 °C with a significant improvement in pH stability.

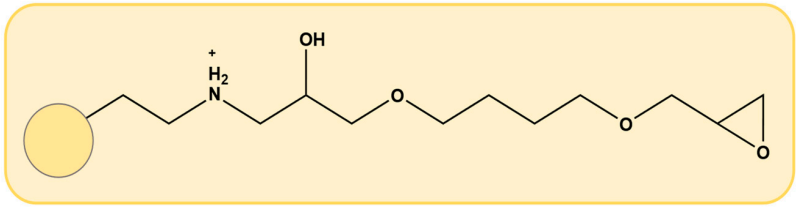


Figure 8. The structure of Sepabeads EC–HFA.

The enzyme retained 75% activity with no significant loss after more than 2 weeks in a packed–bed reactor at 60 °C [36,50]. Studies have shown that the optimal temperature of SPase cross–linked enzyme aggregates (CLEAs) from *Bifidobacterium adolescentis* is 17 °C higher than that of the soluble enzyme, as illustrated in Figure 9.

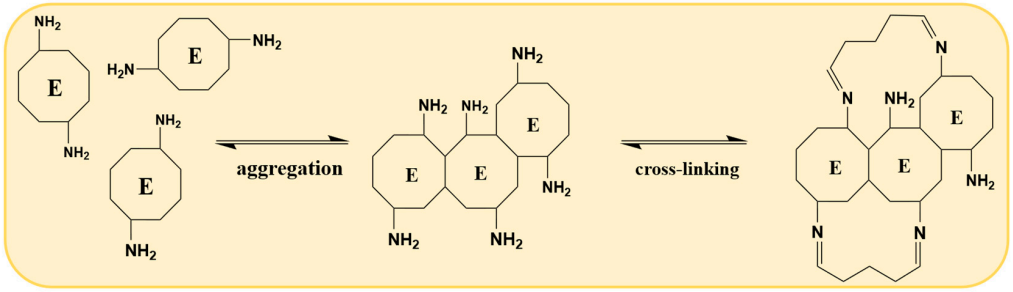


Figure 9. General scheme for the production of cross–linked enzyme aggregates (CLEAs).

Additionally, the immobilized enzyme maintained full activity after 1 week of incubation at 60 °C, demonstrating excellent thermostability [43]. Wim et al. used α–glucosyl glycerol imprinting and glutaraldehyde cross–linking to double the specific activity of SPase for glycerol as an acceptor substrate while also showing excellent stability at 60 °C. This process can be carried out in an aqueous environment to generate a new enzyme formulation called iCLEA with the preparation method shown in Figure 10 [52].

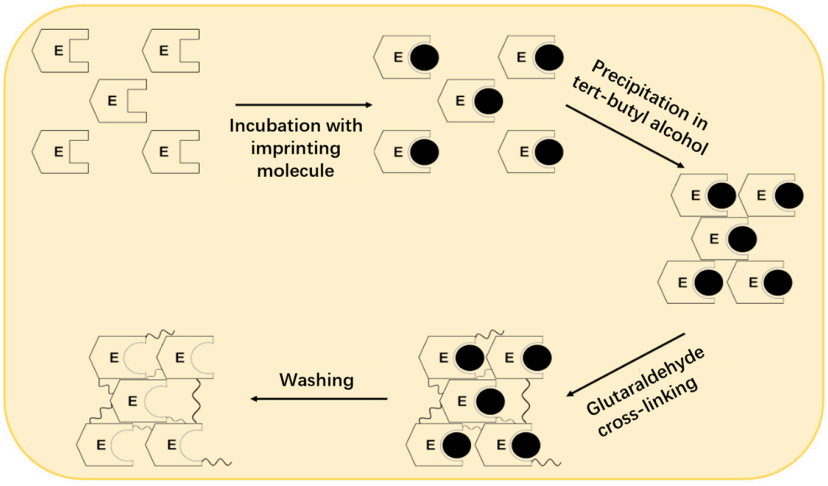


Figure 10. General scheme for the production of imprinted cross–linked enzyme aggregates (iCLEAs). Note: E represents protein and black sphere represents imprinted images.

Although immobilization can enhance enzyme thermostability and extend enzyme activity duration, the process is time–consuming and costly, making it unsuitable for large–scale industrial applications [37]. Microstructured reactors are an emerging tool for developing biocatalytic conversions, where enzymes are fused with the silicon–binding module Zbasic2 to direct high–affinity attachment to glass microchannel walls. This

approach doubled the efficiency of immobilized SPase, and even after 690 reactor cycles, the enzyme maintained approximately 70% activity, offering valuable insights for enzyme microreactor applications in high–performance biocatalytic engineering [51].

In summary, residues affecting thermostability are usually located far from the active site, and if near the active center, they are often protected by a hydrophobic region formed by other amino acid residues. In addition to mutating residues, adding hydrogen bonds and disulfide bonds [60], and utilizing immobilization techniques can also improve protein thermostability. Currently, a series of widely applied modification strategies and techniques have emerged, ranging from directed evolution to semi–rational and rational design, with an increasing reliance on machine learning [61]. Hence, the application of artificial intelligence in protein design and modification must be carefully and reasonably applied, using it to develop proteins optimized for industrial use.

3.2. Transglycosylation Activity Enhancement of SPase

Certain natural small–molecule drugs possess potent antioxidant, anti–inflammatory, and anticancer effects; however, their poor water solubility and bioavailability limit their use. Glycosylation can overcome these limitations, dramatically improving their solubility, stability, bioavailability, and pharmacological efficacy [20]. SPase can synthesize a range of glycoside compounds from sucrose under mild conditions, but achieving specificity and regioselectivity is still a challenge [62]. Site–directed mutagenesis can enhance the selectivity and activity of SPase in glycoside synthesis. The three–dimensional structure of a protein determines its biological function, which is governed by its amino acid sequence. For most enzymes, a few key amino acid residues in the catalytic pocket are responsible for their catalytic functions, including substrate specificity and catalytic efficiency [63]. The active site of the enzyme governs the entry of substrates and solvents. Altering the active site on the loop of SPase through mutagenesis can modify its selectivity [64]. Current methods to enhance transglycosylation activity primarily include loop structure modification, directed evolution, and other protein engineering strategies, as shown in Table 3.

Table 3. Modification of SPase transglycosylation activity based on protein engineering.

Sources Microorganism	Site	Results	Ref.
Bifidobacterium adolescentis	L341I–Q345S	The selectivity of kojibiose was 95%.	[4]
Bifidobacterium adolescentis	Q345F	Produces a mixture of maltose and rare brown sugar.	[5]
Bifidobacterium adolescentis	Q345F/P134D	Effectively increases the control of SPase on the selectivity of (+)– catechin glycosylated regions.	[21]
Bifidobacterium adolescentis	Q345F	The glycosylation rate of aromatic receptors reached up to 97%.	[65]
Bifidobacterium adolescentis	Q345F	Mutations can reversibly shift the structural domain of the active site.	[66]
Bifidobacterium adolescentis	Q345F	Conformational changes in the active site of the mutant are greater than in the natural enzyme.	[67]
Bifidobacterium adolescentis	R135Y–342G–Y344Q–Q345F	The catalytic efficiency (kcat/km) of the synthesis of brown sugar has been increased by 68 times.	[68]
Bifidobacterium breve	L343F	Reduced impurities I and III by 63.9 and 100%, respectively, without affecting the transglycosylation activity.	[69]
Bifidobacterium breve	L341V/L343F	L–AA conversion rate reaches 64%.	[70]
Thermoanaerobacterium thermosaccharolyticum	R134A	The ability of binding to macromolecular receptors increased.	[71]
Bacteria Mediterranean Alternaria	P140D	The pattern of preferential binding of (+)– catechin by AmSP–P140D favors glycosylation on the 4′(OH4′) hydroxyl group.	[72]
Leuconostoc mesenteroides	K138C	The maximum production of αGG by these combined strategies reached 351.8 $g \cdot L^{-1}$ with a 98% conversion rate from 1.4 M sucrose and 3.5 M glycerol in a 5–L bioreactor.	[73]

3.2.1. Enhancing the Transglycosylation Activity of SPase by Protein Engineering

Influence of Q345 Site on the Transglycosylation Activity of SPase

Michael et al. proposed a new multifunctional receptor binding site, marking the first instance of active site remodeling through domain shifting. In the design of *Ba*SP, since Gln345 is near the receptor binding site (+1 position), a Phe345 mutation was introduced to form a receptor π–π stacking interaction (Figure 11).

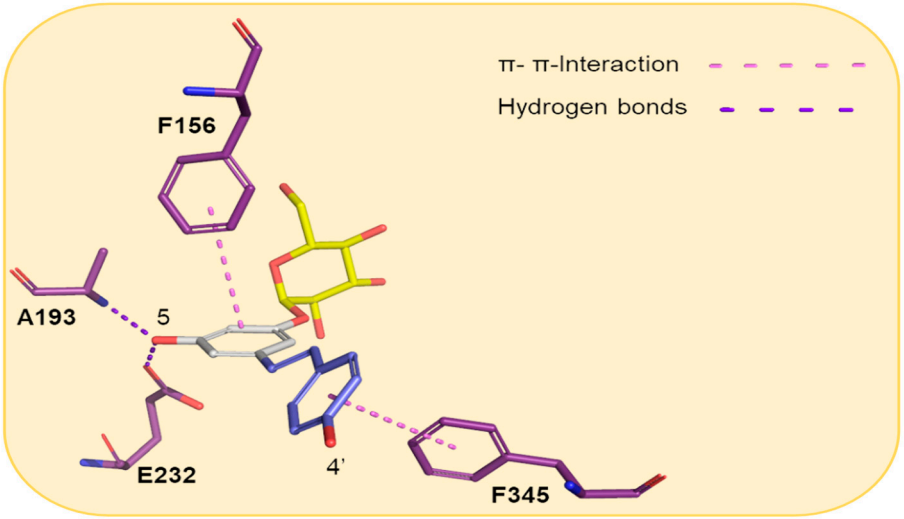


Figure 11. p–p–interactions: the A–ring of the resveratrol moiety (gray) is stabilized via hydrogen bonds to Ala193 and Glu232 and displays T–shape p–p–interactions to Phe156 (741 angle between the aromatic rings); the B–ring and the conjugated double bond (blue) undergo p–p–interactions with Phe345 (88°).

The domain shift expanded the active site, doubling its volume, and allowing the mutant to bind larger molecules like quercetin and resveratrol [18]. Further studies revealed that the Q345F mutation caused a reversible shift in the active site domain (Figure 12) [65]. Molecular dynamics simulations and analysis of both the Q345F mutant and wild–type *Ba*SP were conducted to understand how the Q345F mutation achieves 97% glycosylation selectivity for resveratrol. The study revealed that the Q345F mutant had an expanded active site and structural changes. The interactions between the catalytic triad (Asp192, Glu232, Asp290) and two water molecules at the active site were critical for stabilizing the transition state (Figure 13) [66].

This mutation also altered the products of the enzyme with the mutant producing a mixture of maltose and rare nigerose rather than the maltose and kojibiose mixture produced by wild– type *Ba*SP [5]. Single–point mutations do not always yield positive results; hence, multi–point mutations are necessary. Through bioinformatics prediction and analysis, the Q345F/P134D mutation was introduced in *Ba*SP. The P134D mutation resulted in glycosylation at the 3′–OH position, greatly improving glycosylation selectivity for (+)– catechin [21]. Jorick et al. developed a quadruple mutant (R135Y–D342G–Y344Q–Q345F) with greater selectivity for nigerose synthesis in solution and a 68–fold increase in catalytic efficiency. Molecular dynamics simulations revealed that the quadruple mutant′ s receptor site was more flexible than the Q345F mutant [67]. Although many mutants with enhanced transglycosylation activity have been obtained through mutant construction, modification sites near key active sites may result in enzyme activity loss or reduction. Therefore, computational strategies and platforms are needed to identify sites that can effectively enhance transglycosylation activity and reduce the screening workload for mutant libraries [72].

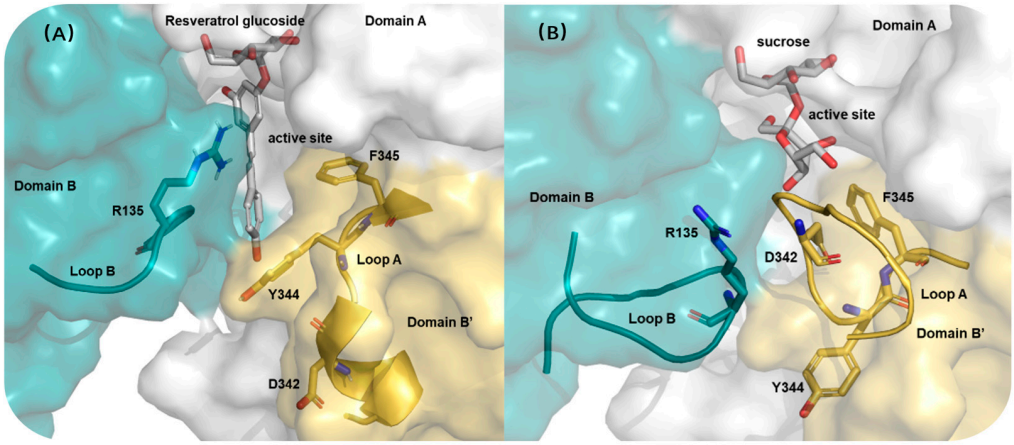


Figure 12. Schematic representation of BaSP Q345F loop conformations. Yellow: Domain B′,Green: Domain B, White: Domain A, Gray: active site cavity. (**A**) Aromatic compound binding conformation of BaSP Q345F (in complex with resveratrol–α–D–glucoside (PDB ID code 5 man)). (**B**) Sucrose binding conformation of BaSP Q345F, sucrose superimposed from 2 gdu. It should be noted that the increase in acceptor site space is due to the domain shift and not a result of the loop rearrangement.

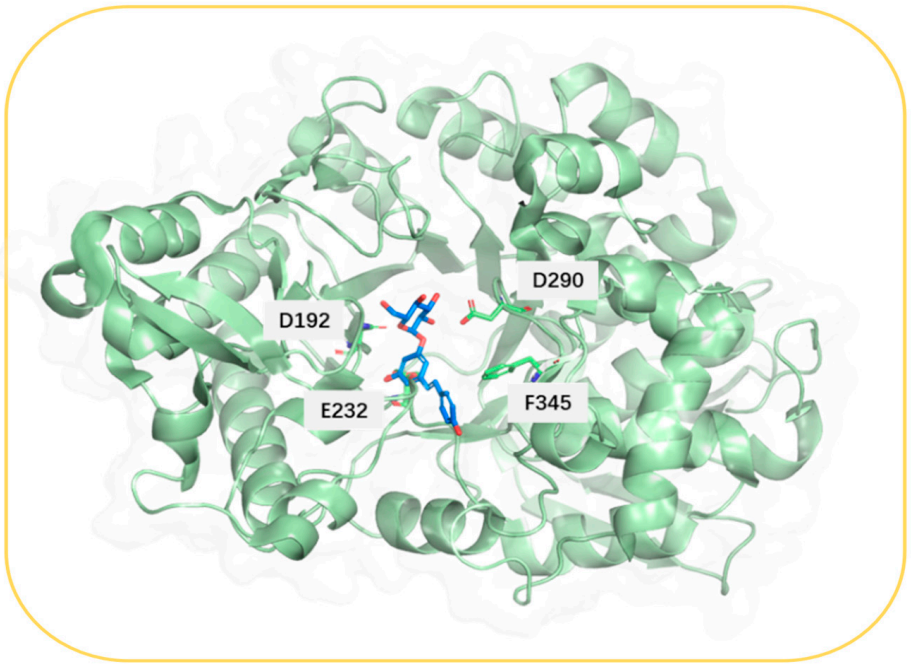


Figure 13. The crystallographic structure of SPase Q345F with PDB ID: 5M9X. The residues of the catalytic triad are shown in green: Glu232, Asp192, and Asp290; mutated Phe345 is also depicted in this color. Resveratrol monoglucoside is represented in light blue.

Mutations at Other Sites by Protein Engineering

Introducing loop modification and cyclic engineering strategies is crucial for enhancing the regioselectivity and substrate specificity of SPase. In addition to the Q345 site, the P134, L341, and L343 sites are also key "hotspots" for regulating the flexibility of the loop. During the SPase–catalyzed synthesis of L–ascorbic acid 2–O–α–d–glucoside (AA–2G) from sucrose and L–ascorbic acid (L–AA), these three hotspots affect the hydrogen bonding network at the active site and the substrate channel entrance, altering the enzyme′ s regioselectivity and substrate specificity. The L341V/L343F mutant achieved nearly 100% control over the selective synthesis of the 2–OH group of L–AA. In a whole–cell conversion system, the L–AA conversion rate of this mutant reached 64%, which is the highest reported level to

date [69]. SPase produces three impurities when synthesizing AA–2G from sucrose and L–AA. To reduce impurity levels, a semi–rational design approach was used to generate the L343F mutant through site–directed mutagenesis, reducing impurities I and III by 63.9% and 100%, respectively, without affecting transglycosylation activity [68], providing greater potential for the industrial production of AA–2G. In addition to AA–2G, the mutations also enhanced the selectivity of *Ba*SP and transglycosylation activity for kojibiose with the *Ba*SP double–mutant L341I–Q345S demonstrating 95% selectivity and minimal loss of activity [4]. Mareike et al. discovered that the R134 residue in TtSP acts as a "gatekeeper", blocking access to the active site and limiting the glycosylation of large receptor molecules. When the R134 residue was replaced with a smaller residue (such as alanine), the R134A mutant exhibited greater affinity for the large receptor resveratrol [70]. Marine Goux et al. mutated the *Alteromonas mediterranea* SPase (*Am*SP) into *Am*SP–Q353F and *Am*SP–P140D, using sucrose as a donor substrate to catalyze the regioselective glycosylation of (+)– catechin. *Am*SP–P140D preferentially glycosylated the 4′ (OH–4′) hydroxyl group of (+)– catechin, while *Am*SP–Q353F favored the 3′ (OH–3′) hydroxyl with both mutants yielding high amounts of specific regioisomers [71]. Peifeng et al. first identified a novel SPase from *Leuconostoc mesenteroides* ATCC 8293 and performed computer–aided engineering to modify the protein, resulting in the K138C mutant with 160% higher activity than the wild type. Structural analysis showed that K138C is a key residue regulating the substrate–binding pocket, significantly influencing its catalytic activity. Moreover, *Corynebacterium glutamicum* was employed for the expression of the mutant and the production of αGG. In a 5–L bioreactor, the highest yield of αGG reached 351.8 $g \cdot L^{-1}$, with a conversion rate of 98%, using 1.4 M sucrose and 3.5 M glycerol as substrates. This represents one of the best achievements in the single–cell biosynthesis of αGG so far, laying the groundwork for its industrial–scale production [72].

3.2.2. Application of Other Strategies in the Modification of SPase Transglycosylation Activity

It is indicated that immobilization strategies not only improve enzyme stability but also enhance enzyme specificity. *Ba*SP from *Bifidobacterium adolescentis* forms cross–linked enzyme aggregates (iCLEA), doubling its specificity for glycerol receptor substrates with selectivity achievable by controlling substrate amounts [52]. SPase′ s transglycosylation activity is severely inhibited by fructose, leading to a sharp decrease in glycosylation rate. A new sucrose batch–feeding strategy effectively reduces the inhibitory effect of fructose [73]. SPase catalyzes the synthesis of αGG from sucrose in the presence of excess glycerol, but excess glycerol must be removed for commercial use. Membrane screening under varying pressures and temperatures identified a suitable membrane with a high αGG rejection rate (<90%) and a low glycerol rejection rate (<5%), ensuring the final product meets functional carbohydrate product standards [74]. The addition of co–solvents can increase enzyme affinity for non–carbohydrate receptors. The evaluation revealed that the ionic liquid IL AMMOENG 101 (Figure 14) is the most effective co–solvent for 28 compounds, including medium and long–chain alcohols, flavonoids, alkaloids, phenolics, and terpenes. Moreover, IL exerts less effect on SPase stability and activity compared to widely used DMSO [75]. The glycosylation of enzymes is affected by the pH of their surrounding environment. It is shown that SPase efficiently catalyzes the 2–O–α–glycosylation of L–AA from sucrose in a pH range of 4.8–6.0, with optimal results at pH 5.2 (Figure 15) [76]. Lastly, the efficiency of transglycosylation reactions depends on the specific SPase employed. By choosing the right substrates and enzymes, and optimizing parameters like substrate concentration and co–solvent pH, SPase–catalyzed transglycosylation reactions can efficiently produce the desired glycosylation products [28].

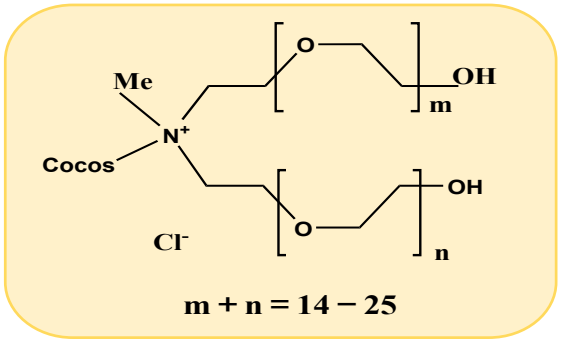


Figure 14. Chemical structure of the ethoxylated quaternary ammonium salt AMMOENG 101.

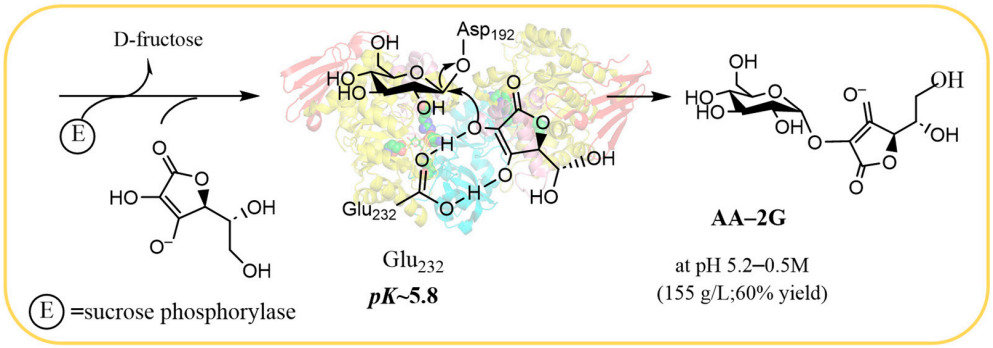


Figure 15. The synthesis of AA–2G from sucrose and L–ascorbic acid in a single−step by SPase.

4. Conclusions

In summary, SPase belongs to the GH13 family, and studies on it are steadily increasing. The first crystal structure of SPase was resolved in 2004, forming the basis for investigating its structure–function relationships and optimizing the enzyme thermostability and substrate specificity for industrial applications. Recent research has concentrated on a few catalytic residues and receptor sites. Studies indicate that distal amino acids influence SPase thermostability, while a small number of residues in the catalytic pocket determine substrate specificity and catalytic efficiency. SPase deactivates quickly at 60 °C, which significantly limits its industrial potential. Various mutation strategies have narrowed the SPase mutant library with semi–rational design significantly enhancing thermostability. Immobilization enhances enzyme thermostability and activity duration, but the process is complex and costly, making it unsuitable for widespread industrial use. Disulfide bonds, ionic interactions, hydrogen bond networks, and polar interactions are crucial for enzyme stability [77]. SPase exhibits broad substrate specificity and can synthesize various glycosides from sucrose with loop mutations further enhancing its selectivity and activity. The geometric conformation and flexibility of the catalytic pocket play a critical role in enzyme stereoselectivity, while the shape of the substrate channel also influences catalytic selectivity [78]. The catalytic pocket of SPase contains two loop structures, and by using crystal structure analysis and (semi–)rational design techniques, the catalytic pocket can be remodeled to regulate SPase function, resulting in industrial enzymes with optimized catalytic properties. Additionally, molecular dynamics (MD), quantum mechanics (QM), and QM/MM methods can elucidate enzyme catalytic mechanisms and guide enzyme design.

In conclusion, recent advances in protein engineering and process improvements have produced many compounds for industrial applications, but more rapid and efficient methods are required to develop new enzyme mutants for producing higher–value compounds. Currently, enzyme modification primarily relies on semi–rational methods such as random or saturation mutations, necessitating more effective modification strategies, including artificial intelligence and machine learning [79,80], to provide more possibilities for the industrial applications of SPase.

Author Contributions: H.Z. and S.M.: writing—original draft, conceptualization, and visualization; T.L.: writing—review and editing; S.W. and H.Z.: supervision and funding acquisition. All authors have read and agreed to the published version of the manuscript.

Funding: This project is funded by the Project Program of Key Laboratory of Industrial Fermentation Microbiology, Ministry of Education, and Tianjin Key Laboratory of Industrial Microbiology, China (No. 2023KF04) and Tianjin College Students Innovation and Entrepreneurship Training Program under grant number 202410069212, 202310069097.

Institutional Review Board Statement: Not applicable.

Informed Consent Statement: Not applicable.

Data Availability Statement: Not applicable.

Conflicts of Interest: The authors declare no conflicts of interest.

References

1. Desmet, T.; Soetaert, W. Enzymatic glycosyl transfer: Mechanisms and applications. *Biocatal. Biotransform.* **2011**, *29*, 1–18. [CrossRef]
2. Stam, M.R.; Danchin, E.G.; Rancurel, C.; Coutinho, P.M.; Henrissat, B. Dividing the large glycoside hydrolase family 13 into subfamilies: Towards improved functional annotations of alpha–amylase–related proteins. *Protein Eng. Des. Sel.* **2006**, *19*, 555–562. [CrossRef] [PubMed]
3. Goedl, C.; Schwarz, A.; Minani, A.; Nidetzky, B. Recombinant sucrose phosphorylase from Leuconostoc mesenteroides: Characterization, kinetic studies of transglucosylation, and application of immobilised enzyme for production of alpha–D–glucose 1–phosphate. *J. Biotechnol.* **2007**, *129*, 77–86. [CrossRef] [PubMed]
4. Beerens, K.; De Winter, K.; Van de Wane, D.V.; Grootaer, C.; Kamiloglu, S.; Miclotte, L.; Van de Wiele, T.V.; Van Camp, J.; Dewettinck, K.; Desmet, T. Biocatalytic Synthesis of the Rare Sugar Kojibiose: Process Scale–Up and Application Testing. *J. Agric. Food Chem.* **2017**, *65*, 6030–6041. [CrossRef] [PubMed]
5. Kraus, M.; Görl, J.; Timm, M.; Seibel, J. Synthesis of the rare disaccharide nigerose by structure–based design of a phosphorylase mutant with altered regioselectivity. *Chem. Commun.* **2016**, *52*, 4625–4627. [CrossRef]
6. Wei, W.; Qi, D.; Diao, M.; Zhaoxin, L.; Lv, F.; Zhao, H. β–galactosidase–catalyzed synthesis of 3–O–β–D–galactopyranosyl–sn–glycerol: Optimization by response surface methodology. *Biocatal. Biotransform.* **2016**, *34*, 152–160. [CrossRef]
7. Goedl, C.; Sawangwan, T.; Mueller, M.; Schwarz, A.; Nidetzky, B. A high–yielding biocatalytic process for the production of 2–O–(α–D–glucopyranosyl)–sn–glycerol, a natural osmolyte and useful moisturizing ingredient. *Angew. Chem. Int. Ed. Engl.* **2008**, *47*, 10086–10089. [CrossRef]
8. Bolivar, J.M.; Luley-Goedl, C.; Leitner, E.; Sawangwan, T.; Nidetzky, B. Production of glucosyl glycerol by immobilized sucrose phosphorylase: Options for enzyme fixation on a solid support and application in microscale flow format. *J. Biotechnol.* **2017**, *257*, 131–138. [CrossRef]
9. Zhou, J.; Jiang, R.; Shi, Y.; Ma, W.; Liu, K.; Lu, Y.; Zhu, L.; Chen, X. Sucrose phosphorylase from Lactobacillus reuteri: Characterization and application of enzyme for production of 2–O–α–d–glucopyranosyl glycerol. *Int. J. Biol. Macromol.* **2022**, *209*, 376–384. [CrossRef]
10. Kwon, T.; Kim, C.T.; Lee, J.H. Transglucosylation of ascorbic acid to ascorbic acid 2–glucoside by a recombinant sucrose phosphorylase from Bifidobacterium longum. *Biotechnol. Lett.* **2007**, *29*, 611–615. [CrossRef]
11. Sugimoto, K.; Nomura, K.; Nishiura, H.; Ohdan, K.; Ohdan, K.; Hayashi, H.; Kuriki, T. Novel transglucosylating reaction of sucrose phosphorylase to carboxylic compounds such as benzoic acid. *J. Biosci. Bioeng.* **2007**, *104*, 22–29. [CrossRef] [PubMed]
12. O′ Neill, E.C.; Field, R.A. Enzymatic synthesis using glycoside phosphorylases. *Carbohydr. Res.* **2015**, *403*, 23–37. [CrossRef] [PubMed]
13. Nakai, H.; Kitaoka, M.; Svensson, B.; Ohtsubo, K. Recent development of phosphorylases possessing large potential for oligosaccharide synthesis. *Curr. Opin. Chem. Biol.* **2013**, *17*, 301–309. [CrossRef] [PubMed]
14. Wang, M.; Wu, J.; Wu, D. Cloning and expression of the sucrose phosphorylase gene in Bacillus subtilis and synthesis of kojibiose using the recombinant enzyme. *Microb. Cell Factories* **2018**, *17*, 23. [CrossRef]
15. Laparra, J.M.; Díez-Municio, M.; Herrero, M.; Moreno, F.J. Structural differences of prebiotic oligosaccharides influence their capability to enhance iron absorption in deficient rats. *Food Funct.* **2014**, *5*, 2430–2437. [CrossRef]
16. Li, Y.; Li, Z.; He, X.; Chen, L.; Cheng, Y.; Jia, H.; Yan, M.; Chen, K. Characterisation of a Thermobacillus sucrose phosphorylase and its utility in enzymatic synthesis of 2–O–alpha–d–glucopyranosyl–l–ascorbic acid. *J. Biotechnol.* **2019**, *305*, 27–34. [CrossRef]
17. Shin, M.H.; Cheong, N.-Y.; Lee, J.-H.; Kim, K.H. Transglucosylation of caffeic acid by a recombinant sucrose phosphorylase in aqueous buffer and aqueous–supercritical CO_2 media. *Food Chem.* **2009**, *115*, 1028–1033. [CrossRef]
18. Kraus, M.; Grimm, C.; Seibel, J. Switching enzyme specificity from phosphate to resveratrol glucosylation. *Chem. Commun.* **2017**, *53*, 12181–12184. [CrossRef]

19. Zhu, X.T.; Tian, Y.Q.; Zhang, W.L.; Zhang, T.; Guang, C.E.; Mu, W.M. Recent progress on biological production of α–arbutin. *Appl. Microbiol. Biotechnol.* **2018**, *102*, 8145–8152. [CrossRef]
20. Gonzalez-Alfonso, J.L.; Ubiparip, Z.; Jimenez-Ortega, E.; Poveda, A.; Alonso, C.; Coderch, L.; Jimenez-Barbero, J.; Sanz-Aparicio, J.; Ballesteros, A.O.; Desmet, T.; et al. Enzymatic Synthesis of Phloretin α–Glucosides Using a Sucrose Phosphorylase Mutant and its Effect on Solubility, Antioxidant Properties and Skin Absorption. *Adv. Synth. Catal.* **2021**, *363*, 3079–3089. [CrossRef]
21. Demonceaux, M.; Goux, M.; Hendrickx, J.; Solleux, C.; Cadet, F.; Lormeau, É.; Offmann, B.; André-Miral, C. Regioselective glucosylation of (+)– catechin using a new variant of sucrose phosphorylase from Bifidobacterium adolescentis. *Org. Biomol. Chem.* **2023**, *21*, 2307–2311. [CrossRef] [PubMed]
22. Kraus, M.; Grimm, C.; Seibel, J. Redesign of the Active Site of Sucrose Phosphorylase through a Clash–Induced Cascade of Loop Shifts. *Chembiochem* **2016**, *17*, 33–36. [CrossRef] [PubMed]
23. Desmet, T.; Soetaert, W. Broadening the synthetic potential of disaccharide phosphorylases through enzyme engineering. *Process Biochem.* **2012**, *47*, 11–17. [CrossRef]
24. Hepworth, L.J.; France, S.P.; Hussain, S.; Both, P.; Turner, N.J.; Flitsch, S.L. Enzyme Cascades in Whole Cells for the Synthesis of Chiral Cyclic Amines. *ACS Catal.* **2017**, *7*, 2920–2925. [CrossRef]
25. Lee, J.H.; Moon, Y.H.; Kim, N.; Kim, Y.M.; Kang, H.K.; Jung, J.Y.; Abada, E.; Kang, S.S.; Kim, D. Cloning and expression of the sucrose phosphorylase gene from *Leuconostoc mesenteroides* in *Escherichia coli*. *Biotechnol. Lett.* **2008**, *30*, 749–754. [CrossRef]
26. Sprogoe, D.; van den Broek, L.A.M.; Mirza, O.; Kastrup, J.S.; Voragen, A.G.J.; Gajhede, M.; Skov, L.K. Crystal structure of sucrose phosphorylase from *Bifidobacterium adolescentis*. *Biochemistry* **2004**, *43*, 1156–1162. [CrossRef]
27. Mirza, O.; Skov, L.K.; Sprogoe, D.; van den Broek, L.A.; Beldman, G.; Kastrup, J.S.; Gajhede, M. Structural rearrangements of sucrose phosphorylase from *Bifidobacterium adolescentis* during sucrose conversion. *J. Biol. Chem.* **2006**, *281*, 35576–35584. [CrossRef]
28. Franceus, J.; Desmet, T. Sucrose Phosphorylase and Related Enzymes in Glycoside Hydrolase Family 13: Discovery, Application and Engineering. *Int. J. Mol. Sci.* **2020**, *21*, 2526. [CrossRef]
29. Mirza, O.; Skov, L.K.; Remaud–Simeon, M.; Potocki de Montalk, G.; Albenne, C.; Monsan, P.; Gajhede, M. Crystal structures of amylosucrase from *Neisseria polysaccharea* in complex with D–glucose and the active site mutant Glu328Gln in complex with the natural substrate sucrose. *Biochemistry* **2001**, *40*, 9032–9039. [CrossRef]
30. Schwarz, A.; Nidetzky, B. Asp–196→Ala mutant of *Leuconostoc mesenteroides* sucrose phosphorylase exhibits altered stereochemical course and kinetic mechanism of glucosyl transfer to and from phosphate. *FEBS Lett.* **2006**, *580*, 3905–3910. [CrossRef]
31. Wiesbauer, J.; Goedl, C.; Schwarz, A.; Brecker, L.; Nidetzky, B. Substitution of the catalytic acid–base Glu237 by Gln suppresses hydrolysis during glucosylation of phenolic acceptors catalyzed by *Leuconostoc mesenteroides* sucrose phosphorylase. *J. Mol. Catal. B Enzym.* **2010**, *65*, 24–29. [CrossRef]
32. Rye, C.S.; Withers, S.G. Glycosidase mechanisms. *Curr. Opin. Chem. Biol.* **2000**, *4*, 573–580. [CrossRef]
33. Vyas, A.; Nidetzky, B. Energetics of the Glycosyl Transfer Reactions of Sucrose Phosphorylase. *Biochemistry* **2023**, *62*, 1953–1963. [CrossRef] [PubMed]
34. Wildberger, P.; Aish, G.A.; Jakeman, D.L.; Brecker, L.; Nidetzky, B. Interplay of catalytic subsite residues in the positioning of alpha–d–glucose 1–phosphate in sucrose phosphorylase. *Biochem. Biophys. Rep.* **2015**, *2*, 36–44. [PubMed]
35. Wildberger, P.; Todea, A.; Nidetzky, B. Probing enzyme–substrate interactions at the catalytic subsite of *Leuconostoc mesenteroides* sucrose phosphorylase with site–directed mutagenesis: The roles of Asp49 and Arg395. *Biocatal. Biotransform.* **2012**, *30*, 326–337. [CrossRef]
36. Cerdobbel, A.; Desmet, T.; De Winter, K.; Maertens, J.; Soetaert, W. Increasing the thermostability of sucrose phosphorylase by multipoint covalent immobilization. *J. Biotechnol.* **2010**, *150*, 125–130. [CrossRef]
37. Cerdobbel, A.; De Winter, K.; Aerts, D.; Kuipers, R.; Joosten, H.J.; Soetaert, W.; Desmet, T. Increasing the thermostability of sucrose phosphorylase by a combination of sequence–and structure–based mutagenesis. *Protein Eng. Des. Sel.* **2011**, *24*, 829–834. [CrossRef]
38. Vieille, C.; Zeikus, G.J. Hyperthermophilic enzymes: Sources, uses, and molecular mechanisms for thermostability. *Microbiol. Mol. Biol. Rev.* **2001**, *65*, 1–43. [CrossRef]
39. Xu, L.; Han, F.; Dong, Z.; Wei, Z. Engineering Improves Enzymatic Synthesis of L–Tryptophan by Tryptophan Synthase from *Escherichia coli*. *Microorganisms* **2020**, *8*, 519. [CrossRef]
40. Liu, Q.; Xun, G.; Feng, Y. The state–of–the–art strategies of protein engineering for enzyme stabilization. *Biotechnol. Adv.* **2019**, *37*, 530–537. [CrossRef]
41. Ashkan, Z.; Hemmati, R.; Homaei, A.; Dinari, A.; Jamlidoost, M.; Tashakor, A. Immobilization of enzymes on nanoinorganic support materials: An update. *Int. J. Biol. Macromol.* **2021**, *168*, 708–721. [CrossRef] [PubMed]
42. Yang, M.; Yang, S.X.; Liu, Z.M.; Li, N.N.; Li, L.; Mou, H.J. Rational Design of Alginate Lyase from *Microbulbife* sp. Q7 to Improve Thermal Stability. *Mar. Drugs* **2019**, *17*, 378. [CrossRef] [PubMed]
43. Cerdobbel, A.; De Winter, K.; Desmet, T.; Soetaert, W. Sucrose phosphorylase as cross–linked enzyme aggregate: Improved thermal stability for industrial applications. *Biotechnol. J.* **2010**, *5*, 1192–1197. [CrossRef]
44. Aerts, D.; Verhaeghe, T.; Joosten, H.J.; Vriend, G.; Soetaert, W.; Desmet, T. Consensus engineering of sucrose phosphorylase: The outcome reflects the sequence input. *Biotechnol. Bioeng.* **2013**, *110*, 2563–2572. [CrossRef]

45. Unsworth, L.D.; van der Oost, J.; Koutsopoulos, S. Hyperthermophilic enzymes–stability, activity and implementation strategies for high temperature applications. *FEBS J.* **2007**, *274*, 4044–4056. [CrossRef]
46. Fujii, K.; Iiboshi, M.; Yanase, M.; Takaha, T.; Kuriki, T. Enhancing the Thermal Stability of Sucrose Phosphorylase from *Streptococcus mutans* by Random Mutagenesis. *J. Appl. Glyosci.* **2006**, *53*, 91–97. [CrossRef]
47. Jochens, H.; Aerts, D.; Bornscheuer, U.T. Thermostabilization of an esterase by alignment–guided focussed directed evolution. *Protein Eng. Des. Sel.* **2010**, *23*, 903–909. [CrossRef]
48. Xia, Y.; Li, X.; Yang, L.; Luo, X.; Shen, W.; Cao, Y.; Peplowski, L.; Chen, X. Development of thermostable sucrose phosphorylase by semi–rational design for efficient biosynthesis of alpha–D–glucosylglycerol. *Appl. Microbiol. Biotechnol.* **2021**, *105*, 7309–7319. [CrossRef]
49. Yang, L.; Peplowski, L.; Shen, Y.; Yang, H.; Chen, X.; Shen, W.; Xia, Y. Enhancing thermostability and activity of sucrose phosphorylase for high–level production of 2–O–α–d–glucosylglycerol. *Syst. Microbiol. Biomanufacturing* **2022**, *2*, 643–652. [CrossRef]
50. De Winter, K.; Cerdobbel, A.; Soetaert, W.; Desmet, T. Operational stability of immobilized sucrose phosphorylase: Continuous production of α–glucose–1–phosphate at elevated temperatures. *Process Biochem.* **2011**, *46*, 2074–2078. [CrossRef]
51. Valikhani, D.; Bolivar, J.M.; Pfeiffer, M.; Nidetzky, B. Multivalency Effects on the Immobilization of Sucrose Phosphorylase in Flow Microchannels and Their Use in the Development of a High–Performance Biocatalytic Microreactor. *ChemCatChem* **2017**, *9*, 161–166. [CrossRef]
52. De Winter, K.; Soetaert, W.; Desmet, T. An imprinted cross–linked enzyme aggregate (iCLEA) of sucrose phosphorylase: Combining improved stability with altered specificity. *Int. J. Mol. Sci.* **2012**, *13*, 11333–11342. [CrossRef] [PubMed]
53. Cheng, Z.; Lan, Y.; Guo, J.; Ma, D.; Jiang, S.; Lai, Q.; Zhou, Z.; Peplowski, L. Computational Design of Nitrile Hydratase from *Pseudonocardia thermophila* JCM3095 for Improved Thermostability. *Molecules* **2020**, *25*, 4806. [CrossRef] [PubMed]
54. Roth, T.; Beer, B.; Pick, A.; Sieber, V. Thermostabilization of the uronate dehydrogenase from *Agrobacterium tumefaciens* by semi–rational design. *AMB Express* **2017**, *7*, 103. [CrossRef]
55. Campeotto, I.; Goldenzweig, A.; Davey, J.; Barfod, L.; Marshall, J.M.; Silk, S.E.; Wright, K.E.; Draper, S.J.; Higgins, M.K.; Fleishman, S.J. One–step design of a stable variant of the malaria invasion protein RH5 for use as a vaccine immunogen. *Proc. Natl. Acad. Sci. USA* **2017**, *114*, 998–1002. [CrossRef]
56. Musil, M.; Stourac, J.; Bendl, J.; Brezovsky, J.; Prokop, Z.; Zendulka, J.; Martinek, T.; Bednar, D.; Damborsky, J. FireProt: Web server for automated design of thermostable proteins. *Nucleic Acids Res.* **2017**, *45*, W393–W399. [CrossRef]
57. Musil, M.; Jezik, A.; Horackova, J.; Borko, S.; Kabourek, P.; Damborsky, J.; Bednar, D. FireProt 2.0: Web–based platform for the fully automated design of thermostable proteins. *Brief. Bioinform.* **2023**, *25*, bbad425. [CrossRef]
58. Weinstein, J.J.; Goldenzweig, A.; Hoch, S.; Fleishman, S.J. PROSS 2: A new server for the design of stable and highly expressed protein variants. *Bioinformatics* **2021**, *37*, 123–125. [CrossRef]
59. Mateo, C.; Grazu, V.; Pessela, B.C.; Montes, T.; Palomo, J.M.; Torres, R.; Lopez-Gallego, F.; Fernandez-Lafuente, R.; Guisan, J.M. Advances in the design of new epoxy supports for enzyme immobilization–stabilization. *Biochem. Soc. Trans.* **2007**, *35 Pt 6*, 1593–1601. [CrossRef]
60. Ni, Z.F.; Li, N.; Xu, P.; Guo, Z.W.; Zong, M.H.; Lou, W.Y. Enhancement of thermostability and catalytic properties of ammonia lyase through disulfide bond construction and backbone cyclization. *Int. J. Biol. Macromol.* **2022**, *219*, 804–811. [CrossRef]
61. Dou, Z.; Sun, Y.; Jiang, X.; Wu, X.; Li, Y.; Gong, B.; Wang, L. Data–driven strategies for the computational design of enzyme thermal stability: Trends, perspectives, and prospects. *Acta Biochim. Biophys. Sin.* **2023**, *55*, 343–355. [CrossRef] [PubMed]
62. Renirie, R.; Pukin, A.; van Lagen, B.; Franssen, M.C.R. Regio–and stereoselective glucosylation of diols by sucrose phosphorylase using sucrose or glucose 1–phosphate as glucosyl donor. *J. Mol. Catal. B Enzym.* **2010**, *67*, 219–224. [CrossRef]
63. Bartlett, G.J.; Porter, C.T.; Borkakoti, N.; Thornton, J.M. Analysis of catalytic residues in enzyme active sites. *J. Mol. Biol.* **2002**, *324*, 105–121. [CrossRef]
64. Sheldon, R.A.; Brady, D.; Bode, M.L. The Hitchhiker′ s guide to biocatalysis: Recent advances in the use of enzymes in organic synthesis. *Chem. Sci.* **2020**, *11*, 2587–2605. [CrossRef]
65. Kraus, M.; Grimm, C.; Seibel, J. Reversibility of a Point Mutation Induced Domain Shift: Expanding the Conformational Space of a Sucrose Phosphorylase. *Sci. Rep.* **2018**, *8*, 10490. [CrossRef] [PubMed]
66. Febres-Molina, C.; Sanchez, L.; Prat-Resina, X.; Jana, G.A. Glucosylation mechanism of resveratrol through the mutant Q345F sucrose phosphorylase from the organism *Bifidobacterium adolescentis*: A computational study. *Org. Biomol. Chem.* **2022**, *20*, 5270–5283. [CrossRef]
67. Franceus, J.; Dhaene, S.; Decadt, H.; Vandepitte, J.; Caroen, J.; Van der Eycken, J.; Beerens, K.; Desmet, T. Rational design of an improved transglucosylase for production of the rare sugar nigerose. *Chem. Commun.* **2019**, *55*, 4531–4533. [CrossRef] [PubMed]
68. Zhou, Y.; Lv, X.; Chen, L.; Zhang, H.; Zhu, L.; Lu, Y.; Chen, X. Identification of Process–Related Impurities and Corresponding Control Strategy in Biocatalytic Production of 2–O–alpha–d–Glucopyranosyl–l–ascorbic Acid Using Sucrose Phosphorylase. *J. Agric. Food Chem.* **2022**, *70*, 5066–5076. [CrossRef] [PubMed]
69. Zhou, Y.; Ke, F.; Chen, L.; Lu, Y.; Zhu, L.; Chen, X. Enhancing regioselectivity of sucrose phosphorylase by loop engineering for glycosylation of L–ascorbic acid. *Appl. Microbiol. Biotechnol.* **2022**, *106*, 4575–4586. [CrossRef]
70. Dirks-Hofmeister, M.E.; Verhaeghe, T.; De Winter, K.; Desmet, T. Creating Space for Large Acceptors: Rational Biocatalyst Design for Resveratrol Glycosylation in an Aqueous System. *Angew. Chem. Int. Ed. Engl.* **2015**, *54*, 9289–9292. [CrossRef]

71. Goux, M.; Demonceaux, M.; Hendrickx, J.; Solleux, C.; Lormeau, E.; Fredslund, F.; Teze, D.; Offmann, B.; Andre-Miral, C. Sucrose phosphorylase from *Alteromonas mediterranea*: Structural insight into the regioselective alpha–glucosylation of (+)–catechin. *Biochimie* **2024**, *221*, 13–19. [CrossRef] [PubMed]
72. Duan, P.; Long, M.; Zhang, X.; Liu, Z.; You, J.; Pan, X.; Fu, W.; Xu, M.; Yang, T.; Shao, M.; et al. Efficient 2–O–alpha–D–glucopyranosyl–sn–glycerol production by single whole–cell biotransformation through combined engineering and expression regulation with novel sucrose phosphorylase from *Leuconostoc mesenteroides* ATCC 8293. *Bioresour. Technol.* **2023**, *385*, 129399. [CrossRef] [PubMed]
73. Zhou, Y.; Gan, T.; Jiang, R.; Chen, H.; Ma, Z.; Lu, Y.; Zhu, L.; Chen, X. Whole–cell catalytic synthesis of 2–O–α–glucopyranosyl–l–ascorbic acid by sucrose phosphorylase from *Bifidobacterium breve* via a batch–feeding strategy. *Process Biochem.* **2022**, *112*, 27–34. [CrossRef]
74. Kruschitz, A.; Nidetzky, B. Removal of glycerol from enzymatically produced 2–α–d–glucosyl–glycerol by discontinuous. *Sep. Purif. Technol.* **2020**, *241*, 116749. [CrossRef]
75. De Winter, K.; Verlinden, K.; Křen, V.; Weignerová, L.; Soetaert, W.; Desmet, T. Ionic liquids as cosolvents for glycosylation by sucrose phosphorylase: Balancing acceptor solubility and enzyme stability. *Green Chem.* **2013**, *15*, 1949–1955. [CrossRef]
76. Gudiminchi, R.K.; Nidetzky, B. Walking a Fine Line with Sucrose Phosphorylase: Efficient Single–Step Biocatalytic Production of l–Ascorbic Acid 2–Glucoside from Sucrose. *Chembiochem* **2017**, *18*, 1387–1390. [CrossRef] [PubMed]
77. Xu, Z.; Cen, Y.K.; Zou, S.P.; Xue, Y.P.; Zheng, Y.G. Recent advances in the improvement of enzyme thermostability by structure modification. *Crit. Rev. Biotechnol.* **2020**, *40*, 83–98. [CrossRef]
78. Kress, N.; Halder, J.M.; Rapp, L.R.; Hauer, B. Unlocked potential of dynamic elements in protein structures: Channels and loops. *Curr. Opin. Chem. Biol.* **2018**, *47*, 109–116. [CrossRef]
79. Mazurenko, S.; Prokop, Z.; Damborsky, J. Machine Learning in Enzyme Engineering. *ACS Catal.* **2019**, *10*, 1210–1223. [CrossRef]
80. Wittmann, B.J.; Yue, Y.; Arnold, F.H. Informed training set design enables efficient machine learning–assisted directed protein evolution. *Cell Syst.* **2021**, *12*, 1026–1045.e7. [CrossRef]

Disclaimer/Publisher's Note: The statements, opinions and data contained in all publications are solely those of the individual author(s) and contributor(s) and not of MDPI and/or the editor(s). MDPI and/or the editor(s) disclaim responsibility for any injury to people or property resulting from any ideas, methods, instructions or products referred to in the content.